

The fragmentation of a line of balls by an impact

BY E. J. HINCH AND S. SAINT-JEAN

*Department of Applied Mathematics and Theoretical Physics,
University of Cambridge, Silver Street, Cambridge CB3 9EW, UK*

Received 7 August 1998; revised 8 December 1998; accepted 5 January 1999

When a long line of stationary touching balls is hit on its end by another ball, the line fragments: some balls fly off at the far end, some in the middle hardly move, and the impacting ball rebounds backwards taking with it some nearby balls. Two laws for the contact force are studied, both elastic and cohesionless: first, a simple law linear in the compression and then the nonlinear $\frac{3}{2}$ -power law of Hertz for touching spheres. For the linear force and for a line of N balls being impacted by a ball at velocity V , $1.5N^{1/3}$ balls fly off from the far end, the furthest at a velocity $1.4VN^{-1/6}$, the others at similar but slower speeds, while the majority rebound, the impacting ball at $-0.13V$ and the n th from the end at a velocity $-0.16Vn^{-5/6}$ at large n . For the nonlinear Hertz law, only two balls fly off from the far end with significant velocities, at $0.986V$ and $0.149V$, the majority hardly move, and a few rebound, the impacting ball at $-0.07V$ and the n th from the end at a velocity $-0.084Ve^{-0.55n}$.

Keywords: impact; impulse wave; fragmentation; rebound; Newton's cradle

1. Introduction

We study the impact of one ball on a long line of balls. While this problem in Newtonian dynamics is so simple to pose, its resolution has some unexpectedly complex details. The fragmentation of larger structures by an impact will be quite complicated.

The behaviour is well known and elementary for the shortest line of just two balls. When ball 1 hits stationary ball 2, there is a brief interaction, during which ball 1 comes to rest and ball 2 takes on the initial velocity of ball 1. This outcome follows directly from the conservation of momentum and energy for the system, assuming as we do that the collision is purely elastic. For longer lines of balls, the two conserved quantities are insufficient to determine the motion. Experience with an executive toy called a 'Newton's cradle', however, suggests that one ball impacting a stationary line will produce one ball flying off the far end with a velocity equal to that of the impacting ball, all the remaining balls becoming stationary. We shall see that this is not exactly what happens.

From the perspective of granular materials, the problem tackled in this paper falls in a gap between the recent research into rapid granular flows and that into quasi-static flows. In studies of rapid granular flow, the duration of collisions between the particles is assumed to be small compared with the interval between collisions, so

that particles only interact in pairs. In studies of quasi-static flows, particles interact with many others all the time, but the inertia of the particles is negligible. The results of this paper depend both on inertia and on multiparticle interactions.

When the line of balls is long, it is natural to think of some effective continuum approximation. Certain aspects, such as the propagation of an impulse wave along the line, are described by a continuum model. Other aspects, however, depend on the discreteness in the system.

Since completing the work for this paper, some related studies have been drawn to our attention. Nesterenko (1983) has examined numerically and analytically the propagation of nonlinear compression pulses along a line of particles. His long-wave theory will be reviewed in § 5*b*. Coste *et al.* (1997) have performed experiments on such solitary waves propagating along a line of precompressed balls. Falcon *et al.* (1998) have further studied a column of spheres colliding with a wall.

2. Governing equations

Consider the motion in one dimension of N equal particles of mass m and diameter d . Let the displacements measured from their initial touching positions be $x_n(t)$, $n = 1, 2, \dots, N$. Thus if the first particle $n = 1$ is the impacting particle at velocity V , the initial conditions are

$$\begin{aligned} x_n(0) &= 0 \quad \text{for all } n, \\ \dot{x}_1(0) &= V \quad \text{and} \quad \dot{x}_n(0) = 0 \quad \text{for } n \geq 2. \end{aligned}$$

The contact force is assumed to be purely elastic and non-cohesive. We consider two cases, a law linear in the compression of the contact and a $\frac{3}{2}$ -power law. Thus we take the force on the n th particle due to its contact with the $(n+1)$ th particle to be

$$-k(x_n - x_{n+1})_+^\alpha, \quad \text{with } \alpha = 1 \text{ or } \frac{3}{2}.$$

The notation $(\cdot)_+$ means take the value of the bracket to be zero if the expression inside is negative, so that the contact force cannot be in tension. The two contact laws arise in Hertz contact theory. For the contact between two solid spheres, $\alpha = \frac{3}{2}$ and $k = d^{1/2}E/3(1 - \nu^2)$, where E is the Young's elastic modulus of the solid balls and ν is the Poisson's ratio. For the contact between two solid cylinders, $\alpha = 1$ and $k = \pi LE/4(1 - \nu^2)$, where L is the length of the cylinders. The contact force is also linear, $\alpha = 1$, for spherical shells so long as they do not dimple, with $k = O(Eh^2/d)$ where h is the thickness of the shell.

Newton's equation of motion for the particles can now be written down as

$$m\ddot{x}_n = k(x_{n-1} - x_n)_+^\alpha - k(x_n - x_{n+1})_+^\alpha$$

for $n = 2, \dots, N-1$; with omission of the first term for the first particle $n = 1$ and omission of the last for $n = N$.

It is convenient for the numerical solution of these equations to non-dimensionalize them. For the linear contact force $\alpha = 1$, the time-scale is $(m/k)^{1/2}$ and the displacement scale is $V(m/k)^{1/2}$. For the nonlinear contact force $\alpha = \frac{3}{2}$, the time-scale is $(m^2/k^2V)^{1/5}$ and the displacement scale is $(m^2V^4/k^2)^{1/5}$. The result of this non-dimensionalization is to render all the coefficients in the governing equations equal

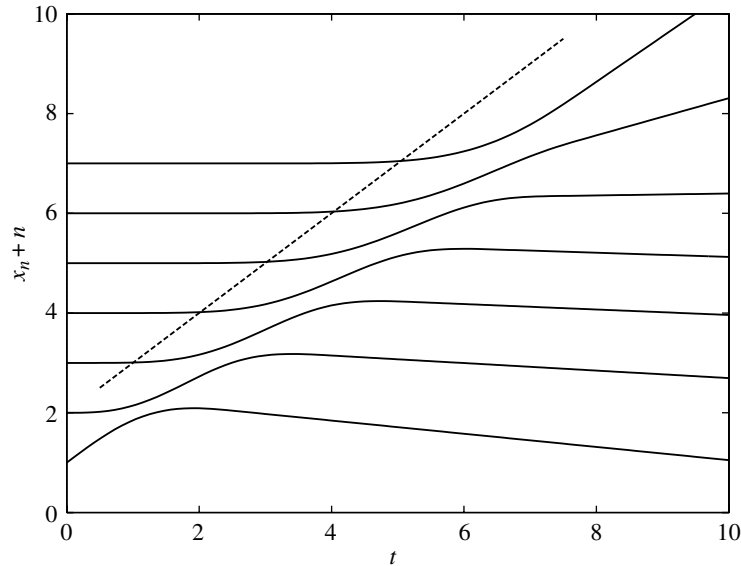


Figure 1. The motion of the particles with a linear contact force. The displacements from the initial positions as a function of time, $x_n(t)$, for all seven particles in a short line. For convenience the displacement of the n th particle has been shifted vertically by n . The dashed line has slope 1, indicating a disturbance propagating down the line at a speed of unity.

to unity:

$$x_n(0) = 0 \quad \text{and} \quad \dot{x}_1(0) = 1, \quad \dot{x}_n(0) = 0 \quad \text{for } n \geq 2, \quad (2.1)$$

$$\ddot{x}_n = (x_{n-1} - x_n)_+^\alpha - (x_n - x_{n+1})_+^\alpha. \quad (2.2)$$

We see that the dynamics of the problem contains no non-dimensional group of parameters. This has the advantage that there is a single solution to be found, and the disadvantage that there is no small parameter to be exploited.

The equations were solved numerically using a fourth-order Runge–Kutta algorithm. In fact the standard algorithm does not give fourth-order accuracy, because the force law changes discontinuously in its derivative between extension and compression. The small non-fourth-order errors only occur occasionally when one particle loses contact with the line, and so the errors are hardly noticeable for short lines. For long lines, however, serious irregularities arise in the small velocities of interest. The numerical method was therefore modified so that if a particle was going to lose contact during the next time-step, then the size of the time-step was adjusted so the separation occurred exactly at the end of the time-step, the appropriate size of the time-step being estimated to second order from a knowledge of x_n , \dot{x}_n and \ddot{x}_n at the beginning of the time-step. To speed up the simulations of some very long lines of particles, another trick was used that exploited the observation that at any one time only a small number of the touching particles had any significant motion.

3. Results for the linear contact force

Figure 1 shows the displacements in time of all the particles in a short line, $N = 7$. The initial slopes are zero except for the lowest curve, which is for the impacting

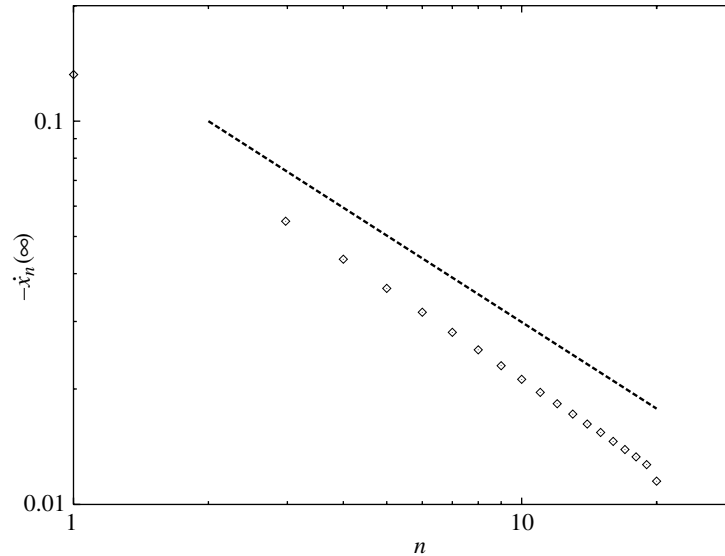


Figure 2. The rebound velocity, $-\dot{x}_n$ after separation, as a function of the position along the line, n , for a line of 25 particles. The dashed line has a slope of $-\frac{3}{4}$.

first particle. The horizontal lines in the top left part of the figure imply that the impact produces a disturbance which propagates down the line at a finite velocity. The dashed line of slope unity indicates that the propagation velocity is constant and of value 1, i.e. one particle per unit of dimensionless time. The dimensional speed in real space is therefore the diameter of the particles divided by the scaling of time, i.e. a velocity $d\sqrt{k/m}$. For the Hertz contact theory between solid cylindrical particles with $k = \pi LE/4(1-\nu^2)$ and $m = \frac{1}{4}\rho\pi Ld^2$, this speed is effectively the speed of sound inside the elastic particles. We therefore have a problem. While quasi-static elasticity theory can still be used within the small contact region to calculate the contact force, it is wrong to treat the particles as rigid masses. One can avoid this hiccup by asking for the solid cylinders to be coated with a soft deformable material that is active within the contact region, while keeping the mass made of a hard rigid material. For the spherical shells, no such problem arises because the propagation speed is less than the sound speed by a factor $\sqrt{h/d}$.

The expression on the right-hand side of the governing equation (2.2) where the particles are touching, $x_{n-1} - 2x_n + x_{n+1}$, is of course the simplest finite-difference approximation to the second-order partial derivative that would be used in a continuum approximation to the problem, $\partial^2 x/\partial n^2$, using a step size $\Delta n = 1$. Thus, where the particles are in contact, the governing equation is an approximation to the wave equation with speed unity. The simplest approximation is, however, known to introduce serious deviations compared with the true wave equation, so we expect the behaviour of our system to be more complicated than just simple wave propagation.

Turning to the right-hand side of figure 1, we see that the curves eventually diverge and the displacements become linear in time. Thus all the contacts are lost, and then with no forces acting all the particles travel at constant non-intersecting velocities. At the top of the right-hand side, we see two particles fly off the far end, the furthest at a velocity just a little less than that of the impacting particle, the next a little slower.

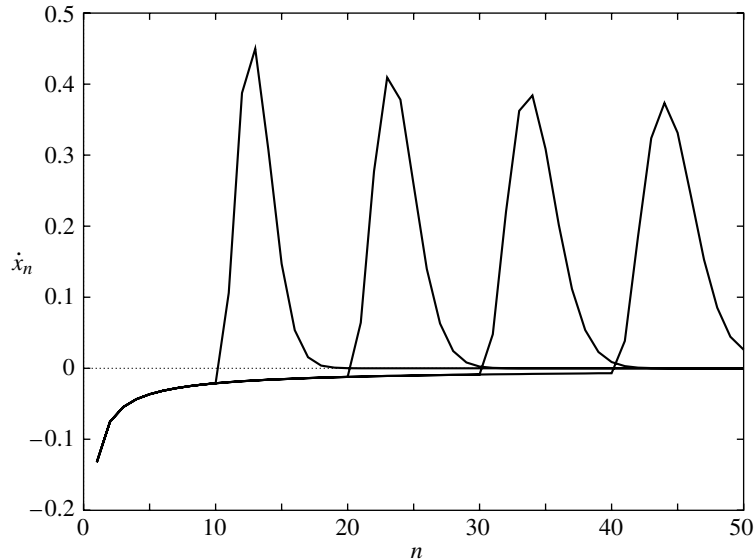


Figure 3. Propagation of an impulse wave. The velocity \dot{x}_n as a function of the position along the line, n , at different times $t = 13.5, 24.5, 35.2$, and 45.7 (when the 10th, 20th, 30th and 40th particles lose contact).

The unexpected feature of figure 1 is that five out of the seven particles eventually rebound backwards. It is not so surprising that the impacting particle rebounds off the line, if one imagines that the initial line of touching particles acts as a continuum elastic body. But after the impacting particle has rebounded, this continuum body repeatedly turns itself into the discrete mass of the next particle plus a continuum body of the remainder, in order for the next particle to bounce off. Note that a pure continuum approximation would not produce any recoil, and so the discreteness of the inertia is important to this behaviour.

We examine further the phenomenon of so many particles rebounding in figure 2, which is for a longer line of 25 particles. Note that 20 particles have a significant rebound velocity, greater than 1% of the initial impact velocity. The dashed line suggests a power-law dependence at large n , $\dot{x}_n(\infty) \propto -n^{-3/4}$. The limited data cannot give the index of the power law accurately, but the slope is clearly less than $-\frac{1}{2}$ and greater than -1 .

An index of less than $-\frac{1}{2}$ means that the contributions of the rebounding particles to the kinetic energy, $\frac{1}{2}\dot{x}_n^2 \propto n^{-3/2}$, converge on summation. In fact we find numerically that only 4% of the impacting kinetic energy is diverted into the rebounding particles. An index greater than -1 is, however, more problematic for the conservation of momentum. The contribution of the rebounding particles to the momentum, $\dot{x}_n \propto -n^{-3/4}$, gives a diverging sum. This suggests that arbitrarily large values of cancelling forward and rebounding momenta would be produced by a sufficiently long line of particles.

While an accurate value of the index cannot be determined from figure 2, it is clear that it is not an easy value to explain. One is used to strange powers occurring in the large highly nonlinear systems that occur in condensed-matter physics. The very simple problem addressed here is, however, nearly linear, and in linear problems

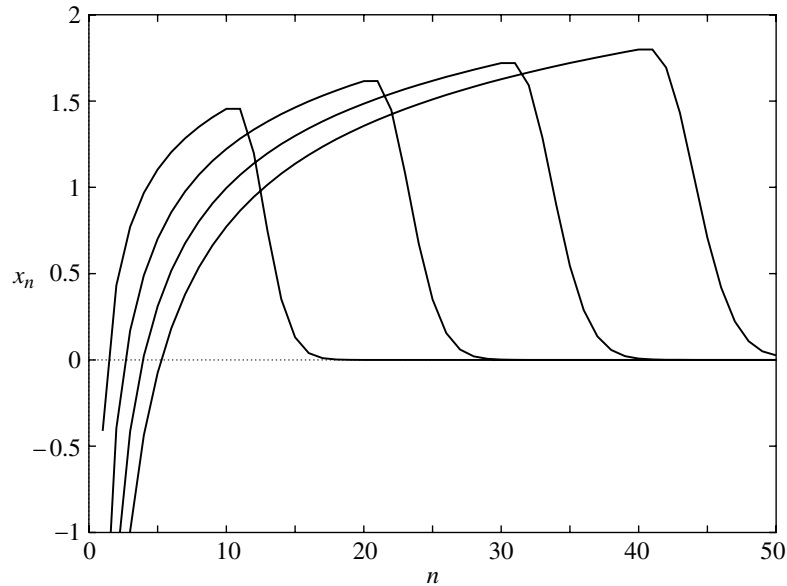


Figure 4. The displacement wave. The displacements x_n as a function of position along the line, n , at different times $t = 13.5, 24.5, 35.2,$ and 45.7 .

one finds at worse something like the $t^{-1/2}$ of diffusion. A theory for the exact value of the index now becomes a central issue to be resolved.

To gain some insight into the behaviour of the fragmenting line of particles, we plot in figure 3 the velocity of the particles as a function of their position along the line at several different times. The strange times are when the 10th, 20th, 30th and 40th particles lose contact. A wave is seen to propagate down the line. Ahead of the wave, the particles are at rest. After the wave has past, the particles take on their rebound negative velocity, which for a given particle does not change in time, and which has a decreasing value for particles further along the line. The form of the wave is that of a single positive pulse, a form which remains roughly the same in time. What clearly does change is the peak of the pulse and its width: the peak velocity decreases slowly in time and the width of the region of activity increases slowly.

Figure 4 is a similar plot to figure 3, except for the displacements rather than the velocities. The displacements are a little more difficult to understand. A wave can still be discerned propagating into a region where the particles are at rest. After the leading edge of the wave has past a particular particle, the particle takes on a negative velocity and so its displacement can be seen to decrease between the different time plots. As the wave propagates down the line, the peak displacement increases slowly, and the width of the leading edge also increases slowly.

4. A theory for the linear contact force

(a) *Energy-conserving wave*

We begin to build a model of the behaviour for the linear contact force by imposing the constraint on a slowly varying wave that it conserves energy. Suppose that the displacement of the particles, $x_n(t)$, is described by a wave of constant form, which

propagates at speed unity and has an amplitude a and wavelength λ that vary slowly in time, i.e.

$$x_n(t) = a(t)f\left(\frac{n-t}{\lambda(t)}\right). \quad (4.1)$$

Here f describes the form of the wave. Because of the unit velocity of propagation, the slowly varying wavelength $\lambda(t)$ is both the number of active particles at time t and also the duration that one particle is active. The separation of time-scales into fast propagation and slow changes in amplitude and wavelength is appropriate only for long chains. The modelling here is thus an informal asymptotic analysis for long chains using multiple time-scales.

The velocities of the particles are found by differentiating expression (4.1) with respect to time. Treating the slowly varying amplitude and wavelength effectively as constants, we only differentiate the propagation factor $(n-t)$. Thus

$$\dot{x}_n \sim -\frac{a}{\lambda}f'. \quad (4.2)$$

The kinetic energy of the particles in the propagating wave is then

$$\sum \frac{1}{2}\dot{x}_n^2 = \sum \frac{1}{2}\frac{a^2}{\lambda^2}f'^2 \propto \frac{a^2}{\lambda},$$

where we have summed over the λ particles where f' is significantly different from zero.

So long as there are many particles within the wavelength λ we may approximate $x_{n+1} - x_n$ by $(a/\lambda)f'$. The potential energy $\sum \frac{1}{2}(x_{n+1} - x_n)^2$ then also reduces to $\sum \frac{1}{2}(a^2/\lambda^2)f'^2$. Thus we have established an equipartition of energy for the slowly varying propagating wave, a property confirmed by the numerical solutions.

We now require energy to be conserved by the propagating wave. It is found in the numerical solutions for a long line of particles that only 3.78% of the impact energy goes into the rebounding particles, leaving 96.2% in the forward propagating wave. Conserving this forward propagating energy gives one relationship between the wavelength $\lambda(t)$ and the amplitude $a(t)$, namely

$$\lambda \propto a^2. \quad (4.3)$$

Substituting this result into the expression (4.2) for the velocity, we obtain

$$\dot{x}_n \propto a^{-1}. \quad (4.4)$$

The above results are consistent with the general observations of the numerical results: that as the wave propagates the wavelength and the peak displacement change slowly in one direction (increase) the peak velocity changes slowly in the other direction (decreases).

A more exacting test of our modelling is to replot the travelling wave in figure 3, dividing the velocity \dot{x}_n by a^{-1} to test result (4.4) and dividing the distance along the wave n by a^2 to test result (4.3). We take a to be the displacement of the last particle to lose contact, say with $n = n_1$ so $a = x_{n_1}$, which is approximately the particle with the largest displacement at that instant. This replot is given in figure 5, where in addition the waves have been shifted to the left through $(n_1 + 0.25)/a^2$. The small

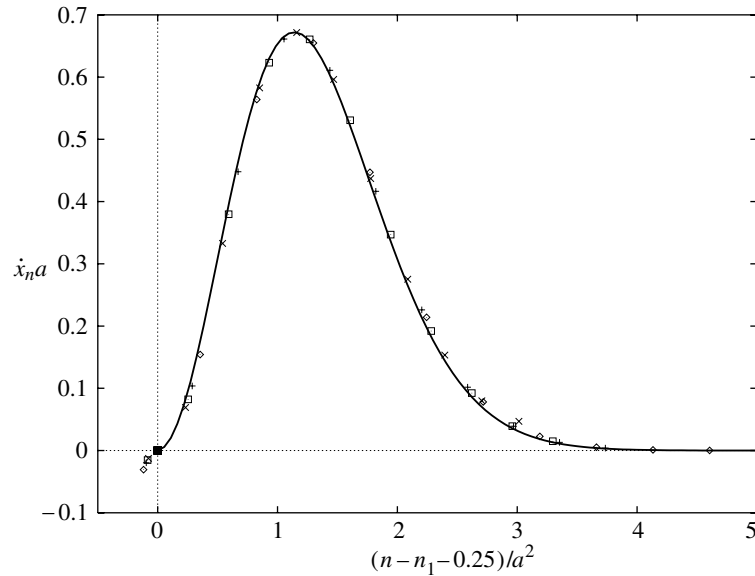


Figure 5. The self-similar impulse wave propagating along the line of particles. The scaled velocity as a function of the scaled position, where n_1 is the last particle not touching others and $a = x_{n_1}$. The different symbols are different times: \diamond , $t = 13.5$; $+$, $t = 24.5$; \square , $t = 35.2$; \times , $t = 45.7$. The continuous curved is the solution to equation (4.9).

correction of 0.25 will be explained in §4e. Figure 5 demonstrates that there is a universal self-similar wave of impulse propagating along the line of particles. Energy conservation has given one relationship between the slowly varying amplitude and wavelength. A further result for either is now needed to complete our modelling.

(b) *Spreading wave*

We return to the idea that the right-hand side of the governing equation (2.2), where the particles are touching, $x_{n+1} - 2x_n + x_{n-1}$, is an approximation to $\partial^2 x / \partial n^2$, and more particularly not a good approximation. It is well known that if one uses this simple finite-difference approximation for the double space derivative in the wave equation, then a solitary wave will erroneously spread out. This is precisely the phenomenon that we wish to characterize. One can analyse this spreading by making a Taylor-series expansion of $x(n \pm 1) = x_{n \pm 1}$ around $x(n) = x_n$, and now keeping more than the leading-order term. Thus one obtains the first correction to the continuum approximation of the simple wave equation:

$$\frac{\partial^2 x}{\partial t^2} = \frac{\partial^2 x}{\partial n^2} + \frac{1}{12} \frac{\partial^4 x}{\partial n^4}. \quad (4.5)$$

The second term on the right-hand side represents the numerical diffusion, which leads to the spreading of the wave.

To solve equation (4.5) for the spreading wave that propagates to the right, we make a coordinate transformation to a frame moving with the propagation velocity of 1. Thus with

$$\nu = n - t$$

equation (4.5) becomes

$$\frac{\partial^2 x}{\partial t^2} - 2 \frac{\partial^2 x}{\partial t \partial \nu} = \frac{1}{12} \frac{\partial^4 x}{\partial \nu^4}.$$

At late times, the first term on the left-hand side becomes negligible, leaving the other two terms to balance. Such a balance is possible only if the scale of the t and ν variations is related by $t\lambda = \lambda^4$. Thus we find the slow variation in the wavelength:

$$\lambda(t) \propto t^{1/3}. \quad (4.6)$$

Combining this with result (4.3), we have the slow variation in the amplitude:

$$a(t) \propto t^{1/6}. \quad (4.7)$$

An alternative derivation of these two results can be obtained by making a steepest-descents analysis of a Fourier-transformation solution of governing equation (2.2) assuming that the particles all remain in contact.

(c) *Rebound velocity*

With the above scaling results for the impulse wave we can now predict the variation of the rebound velocity. The forward momentum in the propagating wave is

$$P = \sum_{\dot{x}_n > 0} \dot{x}_n = \sum_{-f' > 0} -\frac{a}{\lambda} f'.$$

The number of particles with significant positive velocity is proportional to the wavelength λ . Thus

$$P \propto \frac{a}{\lambda} \lambda \propto t^{1/6},$$

using (4.7). The forward momentum in the propagating impulse wave thus increases slowly in time. As the total momentum is conserved, the forward momentum can only increase by regularly ejecting particles moving backwards, as in the propulsion of a rocket. The rate of ejection is equal to the rate that the wave propagates past particles, i.e. the propagation velocity 1. Multiplying this rate of ejection by the velocity of the ejected particles $\dot{x}_n(\infty)$, we find the rate of change in time of the forward momentum:

$$1 \times \dot{x}_n(\infty) = -\dot{P} \propto -t^{-5/6}.$$

Finally, the time at which the n th particle is ejected is equal to n at large n , on account of the unit speed of propagation. Hence

$$\dot{x}_n(\infty) \propto -n^{-5/6}. \quad (4.8)$$

To test result (4.8) we have plotted in figure 6 the rebound velocity $\dot{x}_n(\infty)$ divided by $n^{-5/6}$ as a function of $1/n$. We see that $\dot{x}_n(\infty)n^{5/6}$ tends to a constant -0.158 as $n \rightarrow \infty$. In §3 it was suggested that perhaps $\dot{x}_n(\infty) \propto n^{-3/4}$. That suggestion was based on the limited data of a short line of 25 particles. A second plot in figure 6 of $\dot{x}_n(\infty)n^{3/4}$ is seen to tend to zero rather than a non-zero constant. This demonstrates that $n^{-3/4}$ is not, after all, correct.

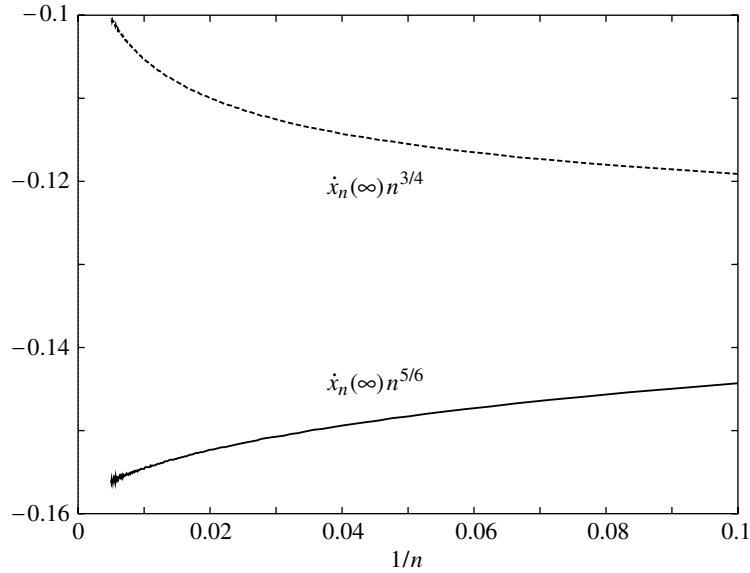


Figure 6. The rebound velocity $\dot{x}_n(\infty)$ divided by $n^{-5/6}$ (continuous curve) and by $n^{-3/4}$ (broken curve) as a function of $1/n$, for a line of 200 particles.

(d) *Similarity solution*

We now derive the analytical form of the universal impulse wave of figure 5. We seek a similarity solution to equation (4.5) for the form of the wave propagating at speed 1 with a wavelength increasing like $t^{1/3}$ and an amplitude increasing like $t^{1/6}$. Thus we pose

$$x_n(t) = t^{1/6} f(\xi) \quad \text{with } \xi = \frac{n-t}{t^{1/3}}.$$

Substituting this into equation (4.5), we obtain

$$f'''' - 8\xi f'' - 4f' = 0, \quad (4.9)$$

ignoring a term $O(t^{-1})$ smaller at large times.

At large positive ξ , the similarity equation (4.9) has four independent solutions, 1, $\xi^{1/2}$, $\exp(\pm \frac{4}{3}\sqrt{2}\xi^{3/2})\xi^{-1}$, the form of the latter two being obtained from a WKB analysis. The requirement that f decays ahead of the wave is therefore equivalent to imposing three boundary conditions. A fourth condition comes from the normalization that the energy (kinetic plus potential) in the wave $\int f'^2 d\xi$ is 96.2% of the impact kinetic energy.

Equation (4.9) was integrated numerically,† shooting backwards from a large $\xi_\infty = 3$, starting on the one decaying solution. The integration was terminated at $\xi_0 = -1.85$ where $f(\xi)$ reaches a maximum. The normalization condition was then applied. This solution of equation (4.9) for the self-similar propagating impulse wave is compared in figure 5 with the earlier simulations of a line of 50 particles. To make the comparison, the velocity $-f'$ is multiplied by the maximum displacement

† After equation (4.9) had been solved numerically, A. M. J. Davis observed that the solution was related to the Airy function, as $f(\xi) = k \int_\xi^\infty \text{Ai}^2(-2^{1/3}y) dy$ (see also Abramowitz & Stegun § 10.4.57).

$f(\xi_0) = 0.956$, and the position along the wave is similarly shifted and rescaled as $(\xi - \xi_0)/f^2(\xi_0)$. The prediction of the wave is good. It can be seen on the figure that at $\xi = \xi_0$ both f'' and f' vanish.

The solution of equation (4.9) also gives a prediction for the magnitude of the rebound velocities. The positive momentum in the self-similar impulse wave is

$$P = t^{1/6} \int_{\xi_0}^{\infty} -f' d\xi = f(\xi_0)t^{1/6}.$$

Differentiating with respect to time, and assuming that the particles rebound regularly at integer times, we obtain

$$\dot{x}_n(\infty) = -\frac{1}{6}f(\xi_0)n^{-5/6}.$$

The value $-\frac{1}{6}f(\xi_0) = -0.159$ should be compared with that of -0.158 obtained in figure 6 from the simulations of a line of 200 particles.

(e) *The 0.25 shift*

The shift of 0.25 in $n - n_1$ used in figure 5 becomes a small correction as $t \rightarrow \infty$. However, at $t = 50$, the appropriate measure $t^{1/3}$ is not very large, and so the ‘small’ correction makes a useful improvement.

The similarity solution in §4d is the leading-order term of an asymptotic solution for large times. It has velocities in the propagating impulse wave of $O(t^{-1/6})$. On the other hand, the rebound velocity of particles losing contact with the line is $O(t^{-5/6})$. Thus there must be an $O(t^{-2/3})$ correction to the leading-order term. We will find this correction in the neighbourhood of the rear of the impulse wave where the particles are losing contact.

Now near $\xi = \xi_0$, equation (4.9), along with $f'(\xi_0) = f''(\xi_0) = 0$, gives the similarity function

$$f(\xi) \sim f(\xi_0)(1 - \frac{2}{3}(\xi - \xi_0)^3).$$

Note that exactly at $\xi = \xi_0$, the leading-order approximation to the velocity, $-t^{-1/6}f'(\xi)$, vanishes.

To the leading-order approximation we add in the neighbourhood of $\xi = \xi_0$ a correction term, $t^{-2/3}$ smaller, with a non-zero velocity, i.e. we consider

$$x_n(t) \sim t^{1/6}f(\xi_0)(1 - \frac{2}{3}(\xi - \xi_0)^3 + \dots) + t^{-1/2}f(\xi_0)\beta(\xi - \xi_0) + \dots,$$

with the constant β to be determined. It is convenient to include the factor $f(\xi_0)$ with β .

Let the value of $n - t$ be δ when particle n loses contact. This quantity is the shift that we seek. We determine the two unknowns δ and β by examining the contact force and the velocity of particle n as it loses contact.

The condition that particle n is losing contact is that the compression between it and the next particle vanishes, i.e. $x_n(t) = x_{n+1}(t)$. This gives at $O(t^{-5/6})$

$$2\delta^2 + 2\delta + \frac{2}{3} - \beta = 0.$$

The condition that particle n loses contact with the rebound velocity $-\frac{1}{6}f(\xi_0)t^{-5/6}$ gives at $O(t^{-5/6})$

$$2\delta^2 - \beta = -\frac{1}{6}.$$

Hence we find the shift used in figure 5 as $\delta = \frac{1}{4}$, along with the coefficient $\beta = \frac{7}{24}$.

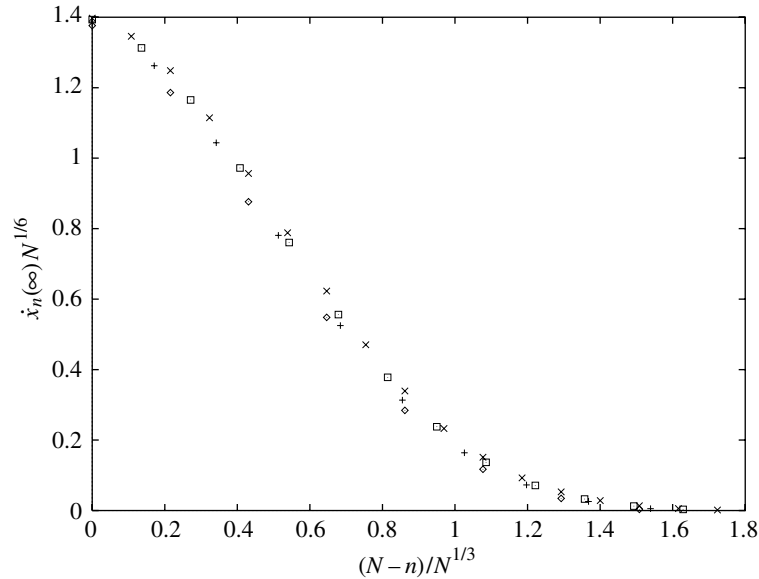


Figure 7. The particles flying off the end of a line of N particles. The scaled final velocity of a particle near the end as a function of the scaled position from the end for different length lines; \diamond , $N = 100$; $+$, $N = 200$; \square , $N = 400$; \times , $N = 800$.

(f) *Finite line*

The above analysis has been of a self-similar impulse wave propagating down effectively an infinite line of particles. If the line is long but finite, containing N particles, then the wave will reach the end at time $t = N$, at which time $O(N^{1/3})$ particles in the wave will have velocities $O(N^{-1/6})$. One would therefore expect $O(N^{1/3})$ particles to fly off the end with such velocities. Figure 7 confirms this by plotting the velocities at which the particles fly off the end divided by $N^{-1/6}$ as a function of their position from the end divided by $N^{1/3}$. The results for four long lines, with $N = 100, 200, 400$ and 800 , collapse onto a single curve. It is seen that $1.5N^{1/3}$ particles have a significant velocity and the fastest at the end has a velocity $1.397N^{-1/6}$. The latter coefficient is twice the peak value 0.703 of $-f'(\xi)$ in figure 5. This doubling is a result of a reflected wave of the same amplitude being emitted from the free end, $\partial x/\partial n = 0$, while the end particle remains in contact, which it does until the peak velocity reaches it. Afterwards, the end particle detaches and an analysis of the reflected wave becomes more difficult.

5. The $\frac{3}{2}$ -power-law contact force

(a) *Results for the fragmentation of a line*

We now change from the linear contact force to the $\frac{3}{2}$ -power law corresponding to Hertz contacts between solid spheres. We shall see that the behaviour is quite different from the case of a linear contact force. Figure 8 shows at different times the displacements of the particles as a function of their position. We first observe that a displacement wave propagates down the line at a constant velocity of 0.841

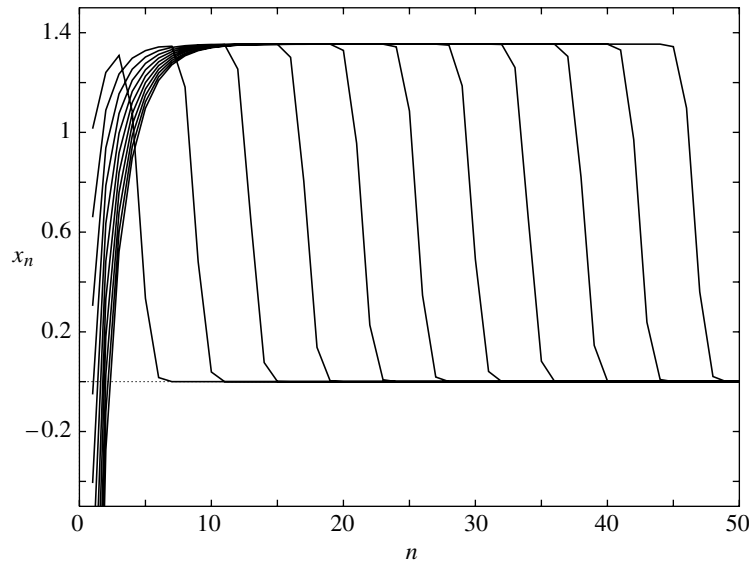


Figure 8. The displacement wave for the $\frac{3}{2}$ -power-law contact force. The displacements x_n as a function of position along the line, n , at different times $t = 5, 10, 15, \dots$. The saturation displacement is 1.354.

in non-dimensional units. The dimensional speed is 0.841 of a particle diameter per unit time-scale, i.e. a speed of

$$0.841d \left(\frac{k^2 V}{m^2} \right)^{1/5} = 0.702 \left[\frac{E^2 V}{\rho^2 (1 - \nu^2)^2} \right]^{1/5},$$

using $k = d^{1/2} E / 3(1 - \nu^2)$ and $m = \frac{1}{6} \rho \pi d^3$. The speed of propagation is therefore slower than the speed of sound c by a small factor $(V/c)^{1/5}$. Hence it is possible to use quasi-static elasticity theory to calculate the contact force and to treat the masses as rigid.

In contrast to the displacement wave in figure 4 for the linear contact force, where the maximum displacement increases as the wave propagates along the line, the displacement wave saturates for the $\frac{3}{2}$ -power law after a period of adjustment to $t = 15$. The saturated displacement is 1.354 in units of $(m^2 V^4 / k^2)^{1/5} = O(d(V/c)^{4/5})$. This saturation corresponds to a balance between the spreading of the wave that was found previously for the linear contact force and a new sharpening of the wave associated with the nonlinearity. This balance also gives a short, fixed, wavelength of about four active particles. Nesterenko's (1983) long-wavelength analysis of this solitary wave will be reviewed in § 5 b.

As the particles pass through the wavefront, they have a maximum velocity of 0.682 in units of V , and experience a maximum force of 0.640 in units of $k^{2/5} m^{3/5} V^{6/5}$. The sum of the momenta of the particles in the solitary wave is 1.138 in units of mV with total energy 0.497 in units of mV^2 . While the total energy is constant, there is a small exchange of kinetic and potential energies as individual particles enter and leave the wavefront. Being a nonlinear system, the average values of the kinetic and potential energies are not equal, but are 0.276 and 0.221, respectively. The kinetic energy fluctuates between 0.272 and 0.282.

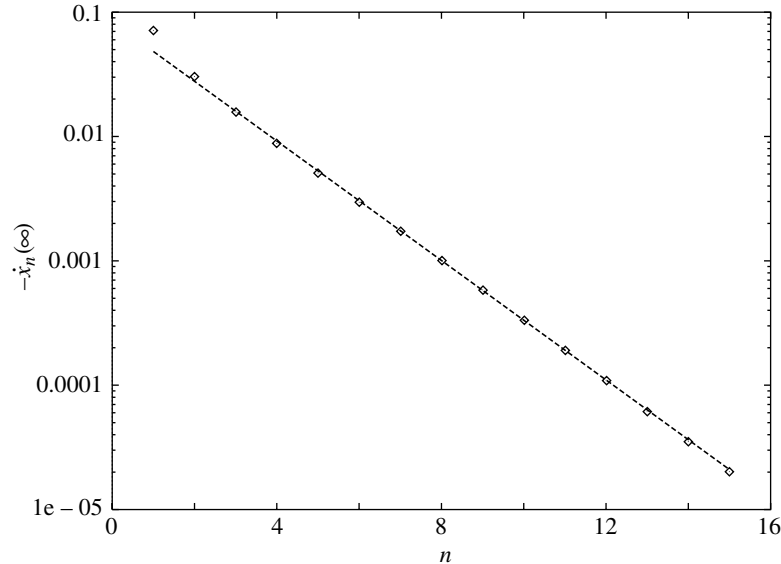


Figure 9. The rebound velocities for the $\frac{3}{2}$ -power-law contact force, as a function of the position along the line, n . The dashed line is $0.084e^{-0.55n}$.

Looking to the left-hand end of figure 8, we see that few particles rebound with the impacting particle. The majority of the particles are displaced through 1.354 and then effectively come to rest. Figure 9 shows for a long line that just three particles rebound with a velocity greater than 1% of the impact velocity. The impacting particle bounces back at -0.0711 , the next at -0.0303 and the third at -0.0158 . Particles 2–15 seem to rebound at a velocity given by $\dot{x}_n(\infty) = -0.084e^{-0.55n}$. This exponential law suggests a quasi-linearized approach to the nonlinear balance between the wave spreading and sharpening. The kinetic energy in the rebounding particles is reduced for the $\frac{3}{2}$ -power-law contact force to just 0.63% of the impact energy. The exponential decay in the rebound velocities means that the total rebound momentum is finite at -0.138 , instead of the $N^{1/6}$ growth for the linear contact force.

When the propagating impulse wave reaches the end of the line, two particles are thrown forward at significant velocities, the furthest at 0.986 and the next at 0.146. The third particle has a velocity of about 0.003. The line needs to contain at least 10 particles to attain these values. A line of five particles produces eventual velocities -0.071 , -0.030 , -0.015 , 0.127 and 0.989.

(b) *Nesterenko's theory for the solitary wave*

From an interest in the absorption of shocks by granular and porous media, Nesterenko (1983) studied the propagation of a compression wave along a line of solid spheres. His governing equations are identical to those used in this paper. He found solitary waves propagating in some numerical solutions. This led him to construct a theory for the solitary waves based on a long-wavelength approximation. The approximation is the same that we used in §4b, of including a further term in the Taylor series of x_{n+1} around x_n .

While the particles are in contact, $x_n > x_{n+1}$, the nonlinear force on particle n from particle $(n + 1)$ is approximated by the first two terms in a Taylor series

$$-(x_n - x_{n+1})^{3/2} \sim -\left(-\frac{\partial x}{\partial n} - \frac{1}{24} \frac{\partial^3 x}{\partial n^3}\right)^{3/2} \sim -\left(-\frac{\partial x}{\partial n}\right)^{3/2} + \frac{1}{16} \left(-\frac{\partial x}{\partial n}\right)^{1/2} \frac{\partial^3 x}{\partial n^3}, \tag{5.1}$$

where these partial derivatives are evaluated at $n + \frac{1}{2}$. Adding the force from particle $(n - 1)$, we obtain the form of the governing equation (2.2) in the long-wavelength approximation:

$$\frac{\partial^2 x}{\partial t^2} = \frac{\partial}{\partial n} \left[-\left(-\frac{\partial x}{\partial n}\right)^{3/2} + \frac{1}{16} \left(-\frac{\partial x}{\partial n}\right)^{1/2} \frac{\partial^3 x}{\partial n^3} \right] + \frac{1}{24} \frac{\partial^3}{\partial n^3} \left[-\left(-\frac{\partial x}{\partial n}\right)^{3/2} \right],$$

where the partial derivatives are now all evaluated at n . A term, which is the third-order derivative of a third-order derivative, has been discarded as a higher-order correction.

Amazingly, Nesterenko presented a simple solution to this nonlinear equation in the form

$$\frac{\partial x}{\partial n} = -A \sin^4 \sqrt{\frac{2}{5}}(n - ct),$$

with velocity of propagation c related to the amplitude A by

$$c^2 = \frac{4}{5} A^{1/2}.$$

Because the right-hand side of the equation vanishes cubically when $\sqrt{2/5}(n - ct)$ approaches a multiple of π , one can construct a solitary wave from one period of the above solution in $0 \leq \sqrt{2/5}(n - ct) \leq \pi$ and taking $\partial x/\partial n$ to vanish identically outside this range.

The net displacement of particles during the passage of the above solitary wave is $(3\pi\sqrt{5}/(8\sqrt{2}))A$. Setting this equal to the 1.354 displacement found in our numerical calculations, we obtain an amplitude $A = 0.727$. With this value of A , Nesterenko's theory predicts a velocity of propagation $c = (2/\sqrt{5})A^{1/4} = 0.826$, which is close to our numerical result of 0.841. The maximum velocity of a particle is predicted to be $Ac = 0.600$, which is 12% lower than our numerical result of 0.682. The maximum of the force, using expression (5.1), is predicted to be $\frac{9}{10}A^{3/2} = 0.558$, which is similarly 13% lower than our numerical result of 0.640. The sum of the momenta of the particles in the solitary wave is predicted to be $(3\pi\sqrt{5}/(8\sqrt{2}))Ac = 1.118$, which is close to our numerical result of 1.138. The kinetic energy of the particles and the potential energy of the springs,

$$\int \frac{2}{5} \left(\frac{\partial x}{\partial n}\right)^{5/2} + \frac{1}{24} \left(\frac{\partial x}{\partial n}\right)^{3/2} \frac{\partial^3 x}{\partial n^3}$$

to be consistent with the expression for the force (5.1), are predicted to be

$$\frac{35\pi\sqrt{2}}{128\sqrt{5}}A^{5/2} = 0.245 \quad \text{and} \quad \frac{28\pi\sqrt{2}}{128\sqrt{5}}A^{5/2} = 0.196,$$

respectively, which are 11% lower than our numerical results of 0.276 and 0.221 for the averages of these fluctuating quantities.

Coste *et al.* (1977) observed solitary waves propagating along a line of touching solid spheres. They found good agreement with Nesterenko's theory for the velocity of propagation as a function of the maximum force exerted between two particles, and less good agreement for the variations of the force with time. It should be noted that they erroneously identified the force with the leading approximation

$$\left(-\frac{\partial x}{\partial n}\right)^{3/2} = A^{3/2} \sin^6 \sqrt{\frac{2}{5}}(n - ct),$$

rather than the more accurate approximation (5.1), which is used in the derivation of the solitary-wave equation. Expression (5.1) gives a force $\frac{3}{5}A^{3/2}(\sin^6 + \frac{1}{2}\sin^4)$. This has a maximum of $0.9A^{3/2}$, which alters the prediction for the propagation velocity by less than 2%. The more accurate expression for the force also decays to zero slightly slower, and this may help to explain the reported poor agreement of the variation of the force with time.

An existence theorem for solitary waves in a discrete chain has been given by Friesecke & Wattis (1994).

(c) *Impact by several particles*

So far we have considered the impact by a single particle on a long line of particles at rest. In this section we consider the impact by several particles. Before the impact, the moving particles have the same velocity and they are touching. Thus we change the initial conditions (2.1) for K -impacting particles to

$$x_n(0) = 0 \quad \text{and} \quad \dot{x}_n(0) = \begin{cases} 1, & \text{if } i = 1, \dots, K, \\ 0, & \text{if } i = K + 1, \dots, N. \end{cases}$$

Figure 10 shows the result of the line of touching particles being impacted simultaneously by two particles. Plotted is the displacement as a function of position along the line at different times. It can be seen that two solitary waves emerge. The faster wave has a saturated displacement of 1.621 and is propagating at a velocity 0.880. The slower wave has an additional displacement of 0.965 and is propagating at 0.773. These two waves are scaled copies of the nonlinear wave in figure 8. They correspond separately to the impact of a single particle at velocities $V = 1.252$ and 0.655, respectively, with the (additional) displacement proportional to $V^{4/5}$ and the propagation velocity proportional to $V^{1/5}$.

As each of the two solitary waves reaches the end of the line, two particles fly forward at significant velocities; at 1.234 and 0.186 from the first and at 0.647 and 0.089 from the second. There follow several binary collisions, e.g. when the faster third particle catches up with the slower second particle, which eventually result in the particles being ordered by decreasing velocity. Note that the pseudo-impacting velocities 1.252 and 0.655 would separately produce particles flying off at significant velocities, at 1.234 and 0.186 and at 0.646 and 0.097. Clearly, there is a small interaction between the waves on the finite length of $N = 50$ used in figure 10.

Figure 11 shows the result of an impact by three particles. Now three solitary waves emerge, again scaled copies of the wave in figure 8. The three waves have (additional) displacements of 1.727, 1.316 and 0.745, corresponding to single-particle impacts at velocities 1.355, 0.965 and 0.474. The solitary waves propagate at velocities 0.894,

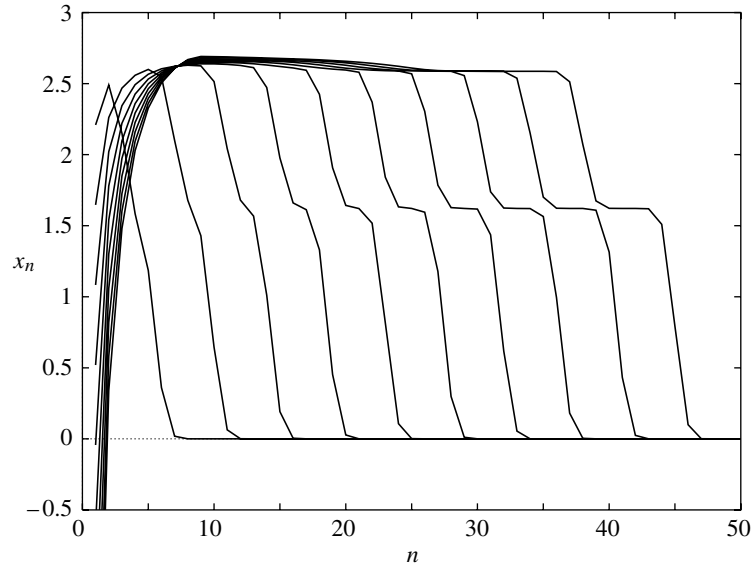


Figure 10. Impact by two particles. The displacements x_n as a function of position along the line, n , at different times, $t = 5, 10, 15, \dots$. All the particles are touching at the time of impact, the first two have the same velocity, 1, while the others are at rest.

0.835 and 0.724. As each wave reaches the end of the line, two particles fly forward; at 1.336 and 0.201 from the first, at 0.953 and 0.132 from the second, and at 0.468 and 0.056 from the third. The pseudo-impacting velocities 1.355, 0.965 and 0.474 would separately produce particles flying off at significant velocities 1.336 and 0.199, 0.951 and 0.142, and 0.467 and 0.070, i.e. there is some interaction between the waves when $N = 100$.

Further numerical calculations with four, five and six impacting particles found the same behaviour of the production of a progression of solitary waves, one wave for each impacting particle. Longer lines are needed for the different solitary waves to separate clearly. The distribution of the amplitudes of these solitary waves, and its dependence on the number of impacting particles, now becomes a subject of interest. At this stage, we have no theoretical ideas for this distribution. The amplitude of the first and fastest solitary wave increases weakly with the number of impacting particles, e.g. the net displacement by the fastest wave is 1.354 for one impacting particle, and increases to 1.621 for two, to 1.727 for three and to 1.775 for four. As each solitary wave ejects two particles when it arrives at the far end, one can examine the distribution of the amplitudes by considering the final velocities of the particles. Figure 12 plots the final velocities of the particles $\dot{x}_n(\infty)$ as a function of their position from the far end $N - n$. It was found that the results came together into a master curve by adding a shift of $\frac{1}{2}$ and by dividing by the number K of impacting particles, i.e. by plotting as a function of $(N - n + \frac{1}{2})/K$. The curve seems to have an exponential decay by one decade for the second particles from each solitary wave, i.e. those with $n = N - K$ to $n = N - 2K$.

For the Hertz $\frac{3}{2}$ -power-law contact force, few particles rebound with one impacting particle. When more particles impact, more rebound, roughly half the number that impact. Figure 13 gives the rebound velocity as a function n of the position from

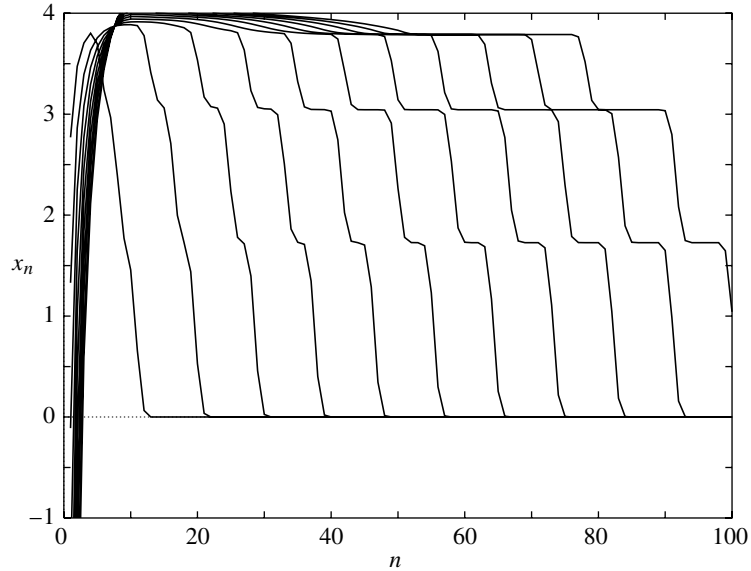


Figure 11. Impact by three particles. The displacements x_n as a function of position along the line, n , at different times, $t = 10, 20, 30, \dots$

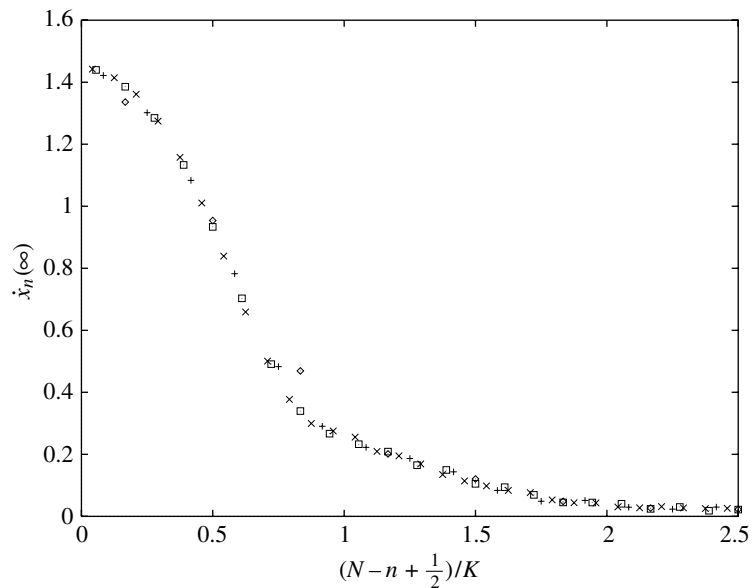


Figure 12. The velocities that particles fly off the far end, as a function of the position along the line, n , with K impacting particles: \diamond , $K = 3$; $+$, $K = 6$; \square , $K = 9$; \times , $K = 12$.

the impact end. Again the results seem to tend to a limit curve when the position is divided by the number of impacting particles. The approach to the limit curve is, however, slow, requiring many more impacting particles to demonstrate the trend.

In this section we have considered several particles impacting a long line. Falcon *et al.* (1998) have performed experiments in which a column of several particles

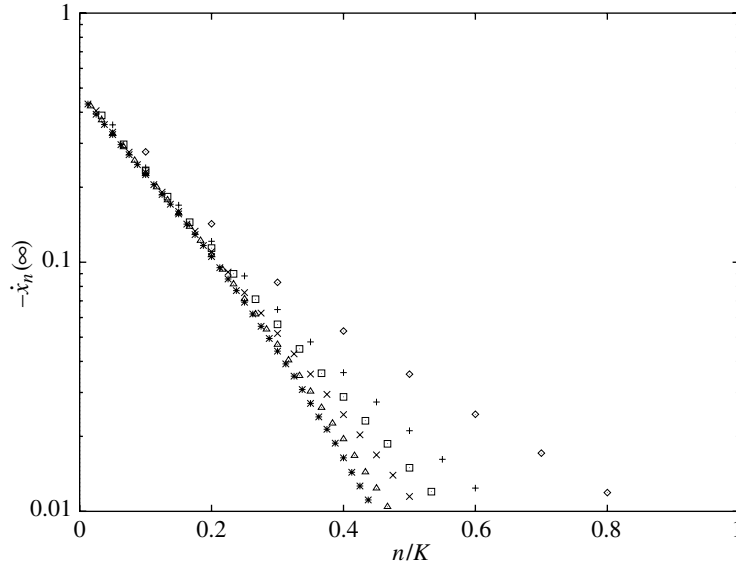


Figure 13. The rebound velocities as a function of the position along the line, n , with K impacting particles: \diamond , $K = 10$; $+$, $K = 20$; \square , $K = 30$; \times , $K = 40$; \triangle , $K = 60$; $*$, $K = 80$.

Table 1. *The final velocities of a line of five spheres*
(The different columns are for different numbers of impacting spheres.)

n	$K = 1$	$K = 2$	$K = 3$	$K = 4$
1	-0.0711	-0.1126	-0.1397	0.0112
2	-0.0303	-0.0420	0.1996	0.8729
3	-0.0145	0.2145	0.7855	1.015
4	0.1270	0.8004	1.042	1.030
5	0.9888	1.140	1.113	1.071

bounces off various types of wall. In the case of a hard wall which deforms less than the particles, their experiments correspond to K particles impacting on an equal number of stationary particles, i.e. $N = 2K$. We have not studied this case.

(d) *Newton's cradle*

The executive toy called a 'Newton's cradle' normally consists of five solid spheres, each suspended from two parallel rails by a pair of light strings. Using two strings confines all of the spheres to move in a single plane, and for swings of small amplitude confines them to a single line. The spheres should be touching in the rest position. If one sphere is moved to the side and then released so it impacts the four other stationary spheres, then one appears to see the sphere at the far end flying off, leaving the remainder stationary. This paper has argued that this is not quite what happens. For a line of five spheres, of the 'stationary remainder' only the second from the far end, sphere $n = 4$, has a significant velocity of 0.13. This can in fact be seen by concentrating attention on the second from the far end, comparing its position with a nearby fixed mark. Alternatively, one can catch the far sphere in midflight,

and see that the other spheres are not still. That the spheres do separate on impact was noted earlier by Herrmann & Seitz (1982).

A further ‘common experience’ with Newton’s cradle is that, if two spheres are moved to the side so that when released they impact together on the other stationary spheres, then two spheres fly off together from the far end. Similarly, three and four spheres impacting simultaneously produce, respectively, three and four spheres flying off together. This ‘common experience’ is only an approximation to the results of a numerical calculation presented in table 1 for the final velocities of a line of five spheres with different numbers of impacting spheres. Knowing what to look for, it is quite easy to observe when two spheres impact five that the central sphere does move and that the two that fly off do so at slightly different velocities and so separate.

S.S.-J. was partly supported by EU grant CHRX-CT93-0354.

References

- Abramowitz, M. & Stegun, I. A. 1965 *Handbook of mathematical functions*. Dover.
- Coste, C., Falcon, E. & Fauve, S. 1997 Solitary waves in a chain of beads under Hertz contact. *Phys. Rev. E* **56**, 6104–6117.
- Falcon, E., Laroche, C., Fauve, S. & Coste, C. 1998 Collision of a 1-D column of beads with a wall. *Eur. Phys. J. B* **5**, 111–131.
- Friesecke, G. & Wattis, J. A. D. 1994 Existence theorem for solitary waves on lattices. *Commun. Math. Phys.* **161**, 391–418.
- Herrmann, F. & Seitz, M. 1982 How does the ball-chain work? *Am. J. Phys.* **50**, 977–981.
- Nesterenko, V. F. 1983 Propagation of nonlinear compression pulses in granular media. *J. Appl. Mech. Tech. Phys. (USSR)* **5**, 733–743.